nature portfolio

https://doi.org/10.1038/s43016-022-00530-x

Supplementary information

A hybrid inorganic–biological artificial photosynthesis system for energy-efficient food production

In the format provided by the authors and unedited

Inventory of Supplementary Information File:

List of Supplementary Tables:

List of Supplementary Figures:

Supplementary References

Supplementary Table 1 | List of state-of-the-art CO_2 and CO electrolysers and their relevant values to this work

Report	Feed	Applied Potential (VCO_2/VCO)	Acetate partial current density (g day^{-1})	Acetate production rate (g day^{-1})	Acetate production rate (g day^{-1} cm^{-2})	Acetate: electrolyte ratio	Fed CO_2 to acetate (%)	Year
This work	CO_2	2.95*/2.3*	51.02	3.43	0.686	0.75	25.39	2021
Ma et al.[61]	CO_2	-0.9 V vs. RHE/N.A.	24.03	0.645	0.645	0.00075	1.67	2020
de Arquer et al.[16]	CO_2	4.5*/N.A.	34.89	0.938	0.938	0.00083	0.97	2020
Romero Cuellar et al.[23]	CO_2	-1 V vs. RHE/-0.8 V vs. RHE	5.43	0.73	0.073	0.0013**	0.53	2020
Ripatti el al.[18]	CO	N.A./2.4*	33.99	0.457	0.457	0.4	N/A	2019
Luc et al.[12]	CO	N.A./-0.8 V vs. RHE	130.92	1.76	1.76	0.005	N/A	2019
Gabardo et al.[13]	CO_2	4.1*/N.A.	6.99	0.941	0.188	0.021	0.61	2019
Jouny et al.[17]	CO	N.A./-0.6 V vs. RHE	106.4	1.43	1.43	0.016	N/A	2018
Lv, J el al.[14]	CO_2	-0.66 V vs. RHE/N.A.	7.22	0.19	0.19	0.002	1	2018

* denotes full cell potential of system (systems with half cell potential full cell was not reported). The value is listed as a positive for the full cell, negative for the half cell as it is a reductive reaction.

** denotes a volume assumed to be 500 ml, based on recirculation rate reported as 200 ml $minute^{-1}$.

Supplementary Table 2 | Measured concentrations and calculated faradaic efficiencies of liquid products detected in effluents after recirculation

		Measured effluent concentrations (M)						Calculated faradaic efficiencies (FE %)				
Effluent	Electrolysis details	KOH	$KHCO_3$	Acetate	Ethanol	Propionate	1-Propanol	Acetate	Propionate	Ethanol	n-Propanol	Ethylene
0.015 M acetate: 1 M KOH*	Direct CO feed	2.0	-	0.030	0.0013	-	0.0004	48.0	0.0	2.4	2.0	16.3
0.077 M acetate: 1 M $KHCO_3$*	Direct CO feed	-	1.0	0.077	0.0130	0.013	0.0099	22.8	1.9	1.8	1.2	19.6
0.2 M acetate: 1 M $KHCO_3$*	Direct CO feed	-	0.5	0.100	0.0020	0.007	0.0007	16.4	0.0	0.4	2.2	15.8
0.38 M acetate: 1 M $KHCO_3$*	Direct CO feed	-	1.0	0.380	0.0130	0.013	0.0099	24.7	2.6	9.5	10.7	30.4
0.4 M acetate: 1 M KOH	CO_2 feed[a]	1.0	-	0.400	0.0500	0.096	0.0580	13.6	9.7	3.4	5.9	36.0
0.476 M acetate: 1 M $KHCO_3$	Direct CO feed	-	1.0	0.476	0.0545	0.012	0.0182	6.9	0.2	0.5	0.3	28.3
0.648 M acetate: 1 M $KHCO_3$	Direct CO feed	-	1.0	0.648	0.0280	0.008	0.0120	5.6	0.3	1.0	0.5	27.9
0.691 M acetate: 1 M KOH	Direct CO feed	2.0	-	1.382	-	0.084	-	28.2	1.7	0.0	0.0	23.8
0.75 M acetate: 1 M KOH	CO_2 feed[b]	1.0	-	0.750	0.0130	0.130	0.0060	33.9	9.0	0.6	0.6	40.2

[a]Without NaOH scrubber

[b]With NaOH scrubber

*Indicates simulated effluent

Supplementary Table 3 | Composition of effluent based media used for microbial growth

	Media component (M)								
Effluent used in media	KOH	$KHCO_3$	Acetate	Ethanol	Propionate	1-Propanol	Organism	Growth observed	Figure utilized in
0.015 M acetate: 1 M KOH*	1.1100	-	0.0167	0.0007	-	0.0002	*Chlamydomonas*	no	Supplementary Fig. 19
0.077 M acetate: 1 M $KHCO_3$*	-	0.2162	0.0167	0.0028	0.0028	0.0021	*Chlamydomonas*	no	Supplementary Fig. 18b-c
0.2 M acetate: 1 M $KHCO_3$*	-	0.2162	0.0167	0.0028	0.0028	0.0021	*Chlamydomonas*	no	Supplementary Fig. 18a
0.38 M acetate: 1 M $KHCO_3$*	-	0.0460	0.0175	0.0006	0.0006	0.0005	*Chlamydomonas*	yes	
0.476 M acetate: 1 M $KHCO_3$	-	0.0350	0.0166	0.0019	0.0004	0.0006	*Chlamydomonas*	yes	Supplementary Fig. 6 and 19
0.648 M acetate: 1 M $KHCO_3$	-	0.0257	0.0166	0.0007	0.0002	0.0003	*Chlamydomonas*	yes	Supplementary Fig. 6
0.691 M acetate: 1 M KOH	0.0241	-	0.0166	-	0.0010	-	*Chlamydomonas*	yes	Figure 3a and supplementary Fig. 6
0.691 M acetate: 1 M KOH*	0.3533	-	0.2442	-	0.0148	-	*Saccharomyces*	yes	Supplementary Fig. 17
0.75 M acetate: 1 M KOH	0.0233	-	0.0175	0.0003	0.003	0.0001	*Chlamydomonas*	yes	Figure 3b-c
0.75 M acetate: 1 M KOH	0.0813	-	0.0609	0.0011	0.0106	0.0005	*Saccharomyces*	yes	Figure 3d-e, Supplementary Fig. 17

*Indicates simulated effluent

Supplementary Table 4 | Previous studies that investigate acetate incorporation into plant metabolites

Plant species	Publication	Method of delivery	Labeled acetate used	Year	Metabolites examined
Tomato	Hill et al.[62]	injected into the fruit	2-^{14}C Acetate	1969	sterol, β-carotene, lycopene
Lettuce	Raymond et al.[63]	liquid incubation	2-^{14}C Acetate	1985	P-esters, citrate, malate, succinate, fumarate, alanine, serine, aspartate, asparagine, glutamine, GABA, leucine/isoleucine
Nicotiana benthamiana	El Tahchy et al.[64]	leaf disc in liquid	^{14}C Acetate	2017	lipids
Arabidopsis thaliana	Fu et al.[65]	grown on supplemented media	2-^{13}C Acetate	2020	histidine, serine, glycine, phenylalanine, alanine, valine, isoleucine, leucine, citrate, glutamate, glutamine, succinate, fumarate, malate, aspartate, asparagine, lysine, methionine, ornithine, proline, GABA
Rice	Tsuda[66]	seedling	2-^{13}C Acetate	2011	poly-β-hydroxybutyrate
Wheat	Tsuda[66]	seedling	2-^{13}C Acetate	2011	poly-β-hydroxybutyrate
Wheat	Williams et al.[67]	leaves incubated in solution	1-^{14}C Acetate	1998	lipids
Corn	Ashworth et al.[68]	suspension cells	1-^{13}C and 2-^{13}C Acetate	1985	palmitate, stearate, linoleate
Soybean	Slack et al.[69]	excised cotyledons	1-^{14}C Acetate	1978	glycerolipids

Supplementary Table 5 | Efficiency of *Saccharomyces* grown with different concentrations of effluent or glucose

Carbon/energy source	Concentration[a] (M)	Energy content[b] (kJ l^{-1})	Yield (g yeast g $glucose^{-1}$)	Yeast produced per area[c] (g yeast m^{-2})	Fold change[d]
Effluent (0.75 M acetate: 1 M KOH)	0.061	53.36	0.1889	6,729	18.24
Effluent (0.75 M acetate: 1 M KOH)	0.122	106.72	0.1122	3,997	10.83
Effluent (0.75 M acetate: 1 M KOH)	0.183	160.08	0.0567	2,020	5.47
Effluent (0.75 M acetate: 1 M KOH)	0.244	213.44	0.0441	1,571	4.26
Glucose	0.019	53.36	0.2429	179	
Glucose	0.038	106.72	0.1594	117	
Glucose	0.057	160.08	0.1392	103	
Glucose	0.076	213.44	0.1195	88	

[a]Concentration of carbon source in media

[b]Energy content from carbon source in media

[c]Yeast produced per area using artificial photosynthesis (effluent) or traditionally (glucose), as calculated above.

[d]Fold change of yeast produced per area using our process, compared to yeast produced per area traditionally with optimized growth of yeast on glucose. (Y_{xS}= 0.5).

Supplementary Table 6 | List of values both calculated and derived for the calculation of the energy efficiency for the two-step electrolyser system

C_{2+} product	Faradaic efficiency (%)	Mass production[a] (g)	Theoretical potential (V)	Electrons passed (n)
Acetate	33.9	0.716	0.73	4
Propionate	9	0.063	1.027	12
Ethanol	0.57	0.0046	1.052	8
n-Propanol	0.62	0.0044	1.027	12
Ethylene	43	0.212	1.049	8
Hydrogen	15.4	N/A	1.23	2

[a]C_{2+} product distribution shown for 1 g of the C_{2+} products

[b]Number of electrons passed from CO per mol produced during CO electrolysis

Supplemental Note

Optimizing CO_2 electrolysis for heterotrophic growth

Some experiments required more effluent than was available, so simulated effluents were generated with the same concentrations of each component. No major difference was observed between organisms grown on electrolyser produced or simulated effluents (Supplementary Fig. 1). No growth was observed for algal cultures in media made with the simulated effluent (0.2 M acetate: 1 M $KHCO_3$), presumably due to inhibition by a component of the effluent (Supplementary Fig. 2a). We performed a "drop-in" experiment of all known effluent components in the highest of productive value ranges to determine the cause of growth inhibition and found the electrolyte salt, $KHCO_3$, was the only inhibitor (Supplementary Fig. 2a-c). Effluent utilizing an alternative electrolyte, KOH (in simulated 0.015 M acetate: 1 M KOH), also did not support growth of *Chlamydomonas* and caused a 50% loss of cell biomass over 16 days (Supplementary Fig. 2d-f). Together these findings, along with previously published data that shows acute exposure to potassium chloride can cause cell death in *Chlamydomonas*[70,71], suggest that the electrolyte (KOH or $KHCO_3$) is causing growth inhibition. To use the effluent for growth directly, the acetate concentration needed to be increased relative to the electrolyte.

To improve the acetate concentration of the effluent, we hypothesized that a highly alkaline environment could increase the selectivity and production rate of acetate[12,17]. The use of 2 M KOH as the supporting electrolyte in the CO electrolyser led to a 3-fold increase in acetate production rate and higher acetate selectivity compared to 1 M $KHCO_3$ (Extended Data Fig. 1c-d, Supplementary Table 3). For biological compatibility, alkaline electrolyte remaining in the effluent has to be neutralized before it is added to growth media. To reduce the concentration of KOH in the final effluent, our electrolysers were designed as an anion exchange membrane electrode assembly. This allows the acetate concentration of the effluent to be controlled by the operating current density (i.e., the reaction rate) and the duration of electrolysis (i.e., the anolyte circulation time). Optimization of these parameters resulted in 99% of the produced acetate to be collected

in the anolyte. Recirculating the electrolyte improved the acetate-to-electrolyte salt ratios, ranging from 0.471 to 0.75 compared to initial electrolyte streams with a ratio of 0.015.

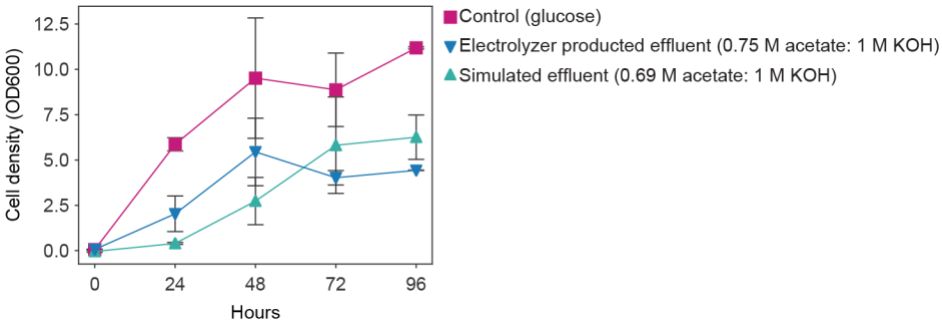

Supplementary Figure 1: Electrolyser produced and simulated effluents used in growth media allow for similar growth.

Optical density (OD) (600 nm) over 96 hours of *Saccharomyces cerevisiae* grown at 30 °C in Yeast-Peptone-Dextrose (YPD) media with glucose (13.7 g l^{-1}), electrolyser produced effluent (0.75 M acetate: 1 M KOH), or simulated effluent (0.69 M acetate: 1 M KOH) as the primary energy and carbon sources. Effluents were added to match the energetic equivalence of 13.7 g l^{-1} glucose (213.44 kJ l^{-1}). Growth data from electrolyser and simulated effluents are from independent experiments conducted at different times which may account for minor differences observed. Each data point represents three replicates. Error bars indicate standard deviations.

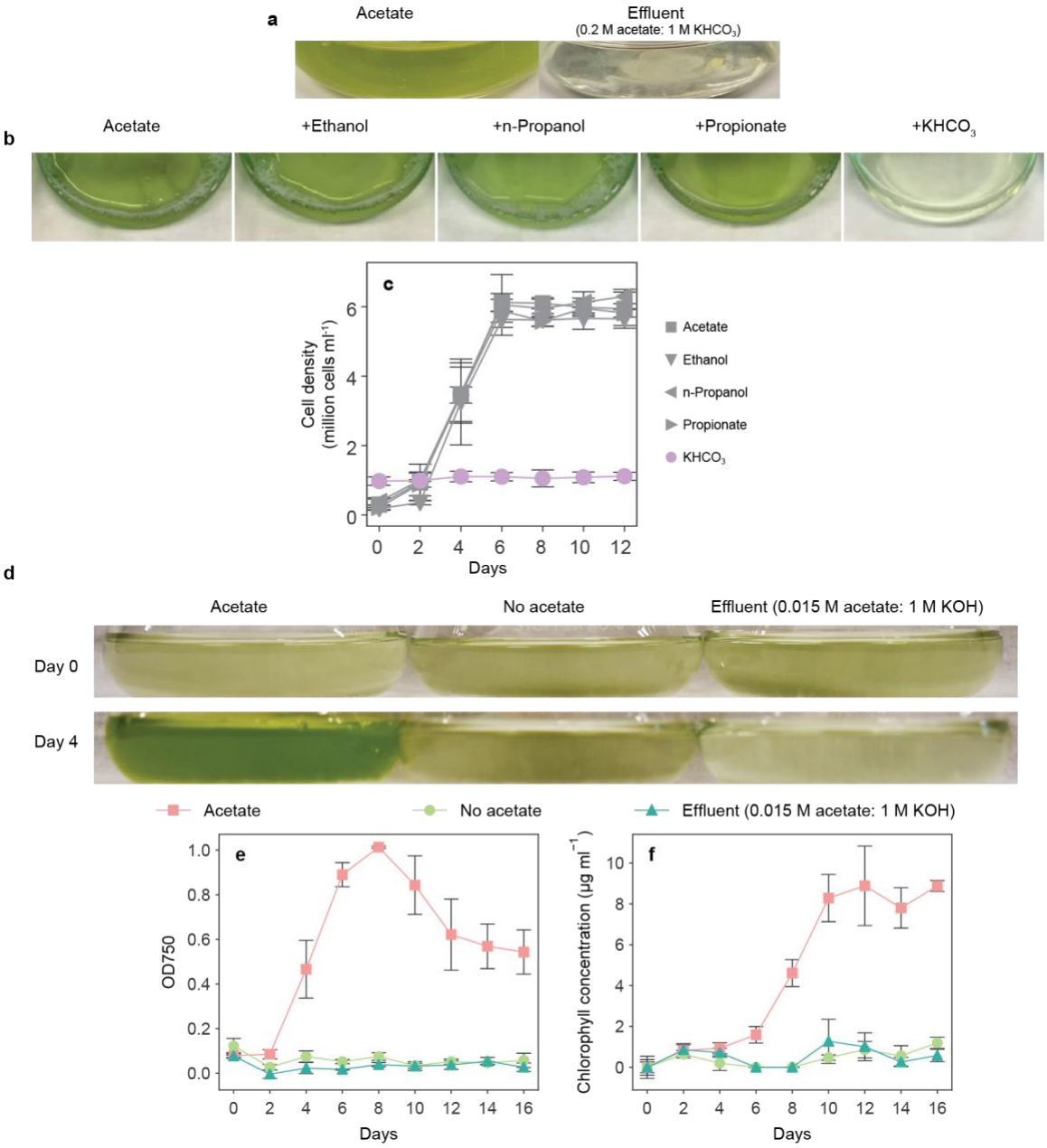

Supplementary Figure 2: The effluent electrolyte hinders *Chlamydomonas* growth and effluent with low acetate-to-electrolyte salt concentration does not support growth of *Chlamydomonas*.

a, Images of *Chlamydomonas* cultures taken after 7 days of growth in darkness, cultures grown with acetate or simulated effluent (0.2 M acetate: 1 M $KHCO_3$). **b, c** *Chlamydomonas* grown in the dark in different media, each containing one component of a proposed “worst-case scenario”

effluent (0.077 M acetate: 1 M $KHCO_3$) containing the lowest concentration of acetate and highest amount of other components. The other effluent components evaluated were ethanol (0.0028 M), n-propanol (0.0021 M), propionate (0.0028 M), and $KHCO_3$ (0.2162 M). (**b**) Images taken on day 12. Cultures were grown in Tris-Acetate-Phosphate (TAP) media with acetate, with acetate and the addition of one effluent component, or with effluent in place of acetate to match the acetate concentration of a typical liquid heterotrophic growth medium (17.5 mM). **d, e, f,** *Chlamydomonas* grown in the dark with simulated effluent (0.015 M acetate: 1 M KOH), acetate, and no acetate. (**d**) Images taken on day 0 and day 4, (**e**) optical density (OD) (750 nm), (**f**) and chlorophyll concentration. Cultures were grown in Tris-Acetate-Phosphate (TAP) media with acetate, without acetate (TP), or with effluent in place of acetate to match the acetate concentration of a typical liquid heterotrophic growth medium (17.5 mM). All media was adjusted to pH 7.2. Each data point represents three replicates. Error bars indicate standard deviations. Images are representative of replicates.

References

61. Ma, W. *et al.* Electrocatalytic reduction of CO_2 to ethylene and ethanol through hydrogen-assisted C–C coupling over fluorine-modified copper. *Nature Catalysis* **3**, 478–487 (2020).
62. Hill, H. M., Shah, S. P. J. & Rogers, L. J. Incorporation of [2-^{14}C]glyoxylate, [2-^{14}C]acetate and [2-^{14}C]mevalonic acid into terpenoids during ripening of tomato fruit. *Phytochemistry* vol. 9 749–755 (1970).
63. Raymond, P., Carre-Nemesio, A. M. & Pradet, A. Metabolism of [^{14}C]ss-glucose and [^{14}C]-acetate by lettuce embryos during early germination. *Physiologia Plantarum* vol. 64 529–534 (1985).
64. El Tahchy, A., Reynolds, K. B., Petrie, J. R., Singh, S. P. & Vanhercke, T. Thioesterase overexpression in *Nicotiana benthamiana* leaf increases the fatty acid flux into triacylgycerol. *FEBS Lett.* **591**, 448–456 (2017).
65. Fu, X., Yang, H., Pangestu, F. & Nikolau, B. J. Failure to Maintain Acetate Homeostasis by Acetate-Activating Enzymes Impacts Plant Development. *Plant Physiol.* **182**, 1256–1271 (2020).
66. Tsuda, H. Generation of poly-β-hydroxybutyrate from externally provided acetate in rice root. *Plant Physiol. Biochem.* **50**, 35–43 (2012).
67. Williams, M., Leech, R. M., Robertson, E. J. & Harwood, J. L. Lipid metabolism in leaves from young wheat (*Triticum aestivum* cv. Hereward) plants grown at two carbon dioxide levels. *J. Exp. Bot.* **49**, 511–520 (1998).
68. Ashworth, D. J., Lee, R. Y. & Adams, D. O. Characterization of acetate and pyruvate metabolism in suspension cultures of *Zea mays* by ^{13}C NMR Spectroscopy. *Plant Physiol.* **85**, 463–468 (1987).
69. Slack, C. R., Roughan, P. G. & Balasingham, N. Labelling of glycerolipids in the cotyledons of developing oilseeds by [1-^{14}C] acetate and [2-^{3}H] glycerol. *Biochem. J* **170**, 421–433 (1978).

70. Vavilala, S. L., Sinha, M., Gawde, K. K. & Shirolikar, S. M. KCl induces a caspase-independent programmed cell death in the unicellular green chlorophyte *Chlamydomonas reinhardtii* (Chlorophyceae). *Phycologia*, **55**(4), 378-392 (2016).
71. Fan, J. & Zheng, L. Acclimation to NaCl and light stress of heterotrophic *Chlamydomonas reinhardtii* for lipid accumulation. *J. Biosci. Bioeng.* **124**, 302–308 (2017).